

## Efficient 3-D wavefield extrapolation with Fourier finite-differences and helical boundary conditions

James Rickett

### Summary

Fourier finite-difference (FFD) migration combines the complementary advantages of the phase-shift and finite-difference migration methods. However, as with other implicit finite-difference algorithms, direct application to 3-D problems is prohibitively expensive. Rather than making the simple  $x - y$  splitting approximation that leads to extensive azimuthal operator anisotropy, I demonstrate an alternative approximation, that retains azimuthal isotropy without the need for additional correction terms.

Helical boundary conditions allow the critical 2-D inverse-filtering step to be recast as 1-D inverse-filtering. A spectral factorization algorithm can then factor this 1-D filter into a (minimum-phase) causal component and a (maximum-phase) anti-causal component. This factorization provides an  $LU$  decomposition of the matrix, which can then be inverted directly by back-substitution. The cost of this approximate inversion remains  $O(N)$  where  $N$  is the size of the matrix.

### Method

Three-dimensional FFD (Ristow and Ruhl, 1994) extrapolation is based on the equation,

$$\frac{\partial P}{\partial z} = i \left[ \sqrt{\frac{\omega^2}{c^2} + \nabla_{x,y}^2} + \left( \frac{\omega}{v} - \frac{\omega}{c} \right) + \frac{\omega}{v} \left( 1 - \frac{c}{v} \right) \frac{\frac{v^2}{\omega^2} \nabla_{x,y}^2}{a + b \frac{v^2}{\omega^2} \nabla_{x,y}^2} \right] P, \quad (1)$$

where  $v = v(x, y, z)$  is the medium velocity,  $c$  is a reference velocity ( $c \leq v$ ), and  $a$  and  $b$  are coefficients subject to optimization. The first term describes a simple Gazdag phase-shift; the second term describes the split-step correction (Stoffa et al., 1990); and the third term describes an additional correction that can be applied as an implicit finite-difference operator (Claerbout, 1985).

In areas with strong lateral velocity variations ( $c/v \approx 0$ ), FFD reduces to a finite-difference migration, while in areas of weak lateral velocity variations ( $c/v \approx 1$ ), FFD retains the steep-dip accuracy advantages of phase-shift migration. As a full-wave migration method, FFD also correctly handles finite-frequency effects.

For constant lateral velocity, the finite-difference term in equation (1) can be rewritten as the following matrix equation,

$$(\mathbf{I} + \alpha_1 \mathbf{D}) \mathbf{q}_{z+1} = (\mathbf{I} + \alpha_2 \mathbf{D}) \mathbf{q}_z \quad (2)$$

$$\mathbf{A}_1 \mathbf{q}_{z+1} = \mathbf{A}_2 \mathbf{q}_z \quad (3)$$

where  $\mathbf{D}$  is a finite-difference representation of the  $x, y$ -plane Laplacian,  $\nabla_{x,y}^2$ . Scaling coefficients,  $\alpha_1$  and  $\alpha_2$ , are complex and depend both on the ratio,  $\omega/v$ , and the ratio  $c/v$ .

The right-hand-side of equation (3) is known. The challenge is to find the vector  $\mathbf{q}_{z+1}$  by inverting the matrix,  $\mathbf{A}_1$ . For 2-D problems, only a tridiagonal matrix must be inverted; whereas, for 3-D problems the matrix becomes blocked tridiagonal. For most applications, direct inversion of such a matrix is prohibitively expensive, and so approximations are required for the algorithm to remain cost competitive with other migration methods.

A partial solution is to split the operator to act sequentially along the  $x$  and  $y$  axes. Unfortunately this leads to extensive azimuthal operator anisotropy, and necessitates expensive additional phase correction operators.

The blocked-tridiagonal matrix of the 3-D extrapolation,  $\mathbf{A}_1$ , represents a two-dimensional convolution operator. Following Rickett et al.'s (1998) approach to factoring the  $45^\circ$  equation, I apply helical boundary conditions (Claerbout, 1998b), to simplify the structure of the matrix, reducing the 2-D convolution to an equivalent problem in one dimension.

For example, through the process illustrated in Figure 1, helical boundary conditions allow the two-dimensional 5-point Laplacian filter,  $d$ , to be expressed as an equivalent one-dimensional filter of length  $2N_x + 1$  as follows

$$d = \begin{bmatrix} & 1 \\ 1 & -4 & 1 \\ & 1 \end{bmatrix} \xrightarrow{\text{helical boundary conditions}} (1, 0, \dots 0, 1, -4, 1, 0, \dots 0, 1)$$

Unfortunately, the complex scale-factor,  $\alpha_1$ , means  $\mathbf{A}_1$  is symmetric, but not Hermitian, so the filter,  $a_1$ , is not an autocorrelation function, and standard spectral factorization algorithms will fail. Fortunately, however, the Kolmogoroff method can be extended to factor any cross-spectrum into a pair of minimum phase wavelets and a delay (Claerbout, 1998a).

With this algorithm, the 1-D convolution filter of length  $2N_x + 1$  can be factored into a pair of (minimum-phase) causal and (maximum-phase) anti-causal filters, each of length  $N_x + 1$ . Fortunately, filter coefficients drop away rapidly from either end, and in practice, small-valued coefficients can be safely discarded.

By reconstituting the matrices representing convolution with these filters, I obtain an approximate *LU* decomposition of the original matrix. The lower and upper-triangular factors can then be inverted efficiently by recursive back-substitution.

While we have only described the factorization for  $v(z)$  velocity models, the method can also be extended to handle lateral variations in velocity. For every value of  $\omega/v$  and  $c/v$ , we precompute the factors of the 1-D helical filters,  $a_1$  and  $a_2$ . Filter coefficients are stored in a look-up table. We then extrapolate the wavefield by non-stationary convolution, followed by non-stationary polynomial division. The convolution is with the spatially variable filter pair corresponding to  $a_2$ . The polynomial division is with the filter pair corresponding to  $a_1$ . The non-stationary polynomial division is exactly analogous to time-varying deconvolution, since the helical boundary conditions have converted the two-dimensional system to one-dimension.

## Examples

Figure 2 compares time-slices through impulses response of FFD migration (with  $c/v = 0.8$ ) for the splitting approximation, (a), and the helical factorization, (b). Figure 3 shows extracts from a three-dimensional FFD depth migration of a zero-offset subset from the SEG/EAGE salt dome dataset.

## REFERENCES

- Claerbout, J. F., 1985, Imaging the earth's interior: Blackwell Scientific Publications.
- Claerbout, J., 1998a, Factorization of cross spectra: SEP-**97**, 337–342.
- Claerbout, J., 1998b, Multidimensional recursive filters via a helix: Geophysics, **63**, 1532–1541.
- Rickett, J., Claerbout, J., and Fomel, S., 1998, Implicit 3-D depth migration by wavefield extrapolation with helical boundary conditions: 68th Ann. Internat. Meeting, Soc. Expl. Geophys., 1124–1127.
- Ristow, D., and Ruhl, T., 1994, Fourier finite-difference migration: Geophysics, **59**, no. 12, 1882–1893.
- Stoffa, P. L., Fokkema, J. T., de Luna Freire, R. M., and Kessinger, W. P., 1990, Split-step Fourier migration: Geophysics, **55**, no. 4, 410–421.

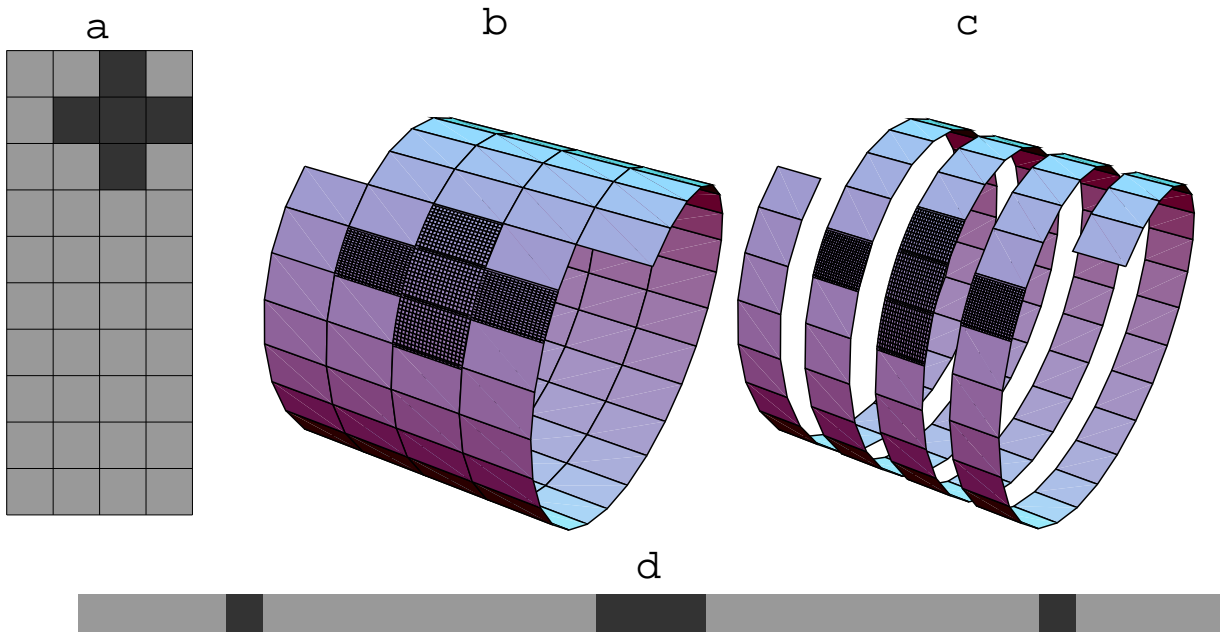


Figure 1: Illustration of helical boundary conditions mapping a two-dimensional function (a) onto a helix (b), and then unwrapping the helix (c) into an equivalent one-dimensional function (d). (Figure by Sergey Fomel).

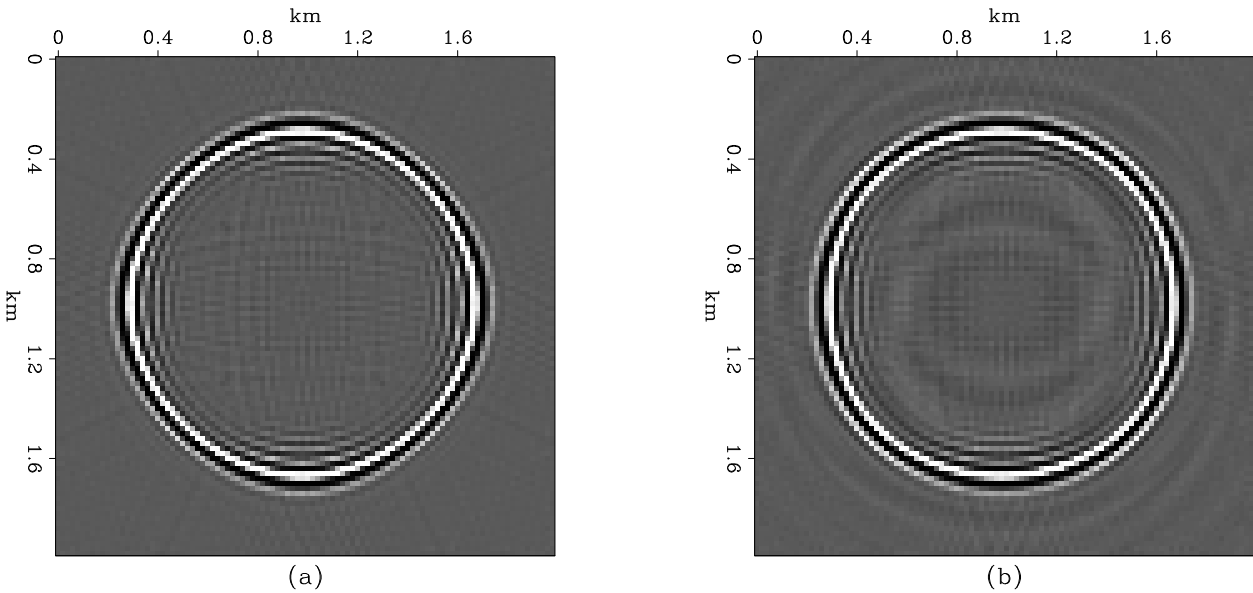


Figure 2: Depth-slices of centered impulse response corresponding to a dip of  $45^\circ$  for  $c/v = 0.8$ . Panel (a) shows the result of employing an  $x - y$  splitting approximation, and panel (b) shows the result of the helical factorization. Note the azimuthally isotropic nature of panel (b).

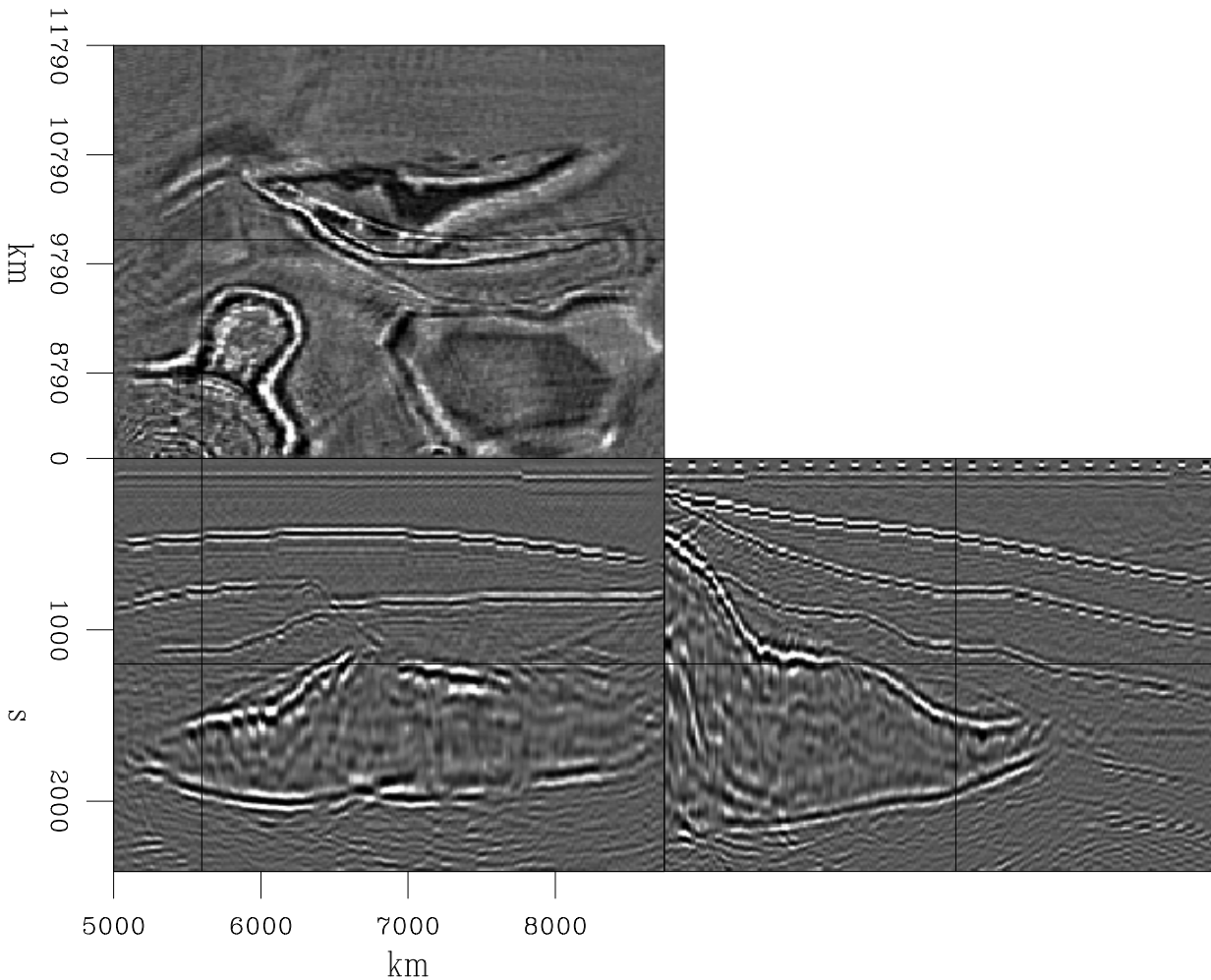


Figure 3: Migration of a three-dimensional zero-offset subset from the SEG/EAGE salt dome dataset by Fourier finite-differences with helical boundary conditions.